pQTL Mendelian randomization analysis combined with single-cell sequencing to identify biomarkers and drug targets for bladder cancer

WENZHI GAO[1], YUE LI[2], ZHIXIN FU[2], ZIHUI GAO[1], YAMING GU[1], XIAOPENG JIA[2], YUQING JIANG[2] and YUEXIAN GUO[2]

[1]Department of Urology, Peking University First Hospital-Miyun Hospital, Beijing 101500, P.R. China;
[2]Department of Urology, The Third Hospital of Hebei Medical University, Shijiazhuang, Hebei 050000, P.R. China

Received March 12, 2025; Accepted August 20, 2025

DOI: 10.3892/mco.2025.2901

Abstract. Despite the development and application of numerous biomarkers and targeted therapeutic approaches for bladder cancer, substantial limitations and challenges persist in its early diagnosis and targeted treatment. As a result, there is an immediate necessity to discover novel biomarkers and develop new targeted drugs. In the present study the association between genes and bladder cancer was analyzed through Mendelian randomization (MR). Sensitivity analysis was conducted to evaluate the reliability of gene causality. Colocalization analysis was used to reduce confounding factors due to linkage disequilibrium and improve the accuracy of causal inference. Validation was performed using quantitative polymerase chain reaction (qPCR) in bladder cancer cell lines. A nomogram model was constructed, and drug sensitivity analysis and single-cell expression typing were conducted to predict survival, select potential therapeutic targets, and detect specific cell types with abundant expression. The results identified seven genes whose predicted levels were associated with bladder cancer risk in the MR analysis. Elevated levels of four genes and decreased levels of three genes were associated with low risk of bladder cancer. All-*trans* retinoic acid-induced differentiation factor (ATRAID) and tripartite motif containing 25 (TRIM25) showed colocalization with SNP.PP.H4 values >0.95, indicating a high likelihood of association with bladder cancer risk. Reverse transcription qPCR validation revealed low expression of ATRAID and TRIM25 in bladder cancer. ATRAID is primarily expressed in fibroblasts and smooth muscle cells, while TRIM25 is highly expressed in endothelial cells. Using clinical data from patients, a model based on ATRAID and TRIM25 demonstrated excellent predictive performance. Furthermore, drug analysis revealed that the expression of ATRAID and TRIM25 is closely associated with the sensitivity to various chemotherapy drugs. In the present study, ATRAID and TRIM25 were identified as two biomarkers linked to the risk of bladder cancer. These findings not only provide new insights into the etiology of bladder cancer but also identify novel targets for the development of biomarkers and therapeutic medications against the disease.

Correspondence to: Professor Yuexian Guo or Professor Yuqing Jiang, Department of Urology, The Third Hospital of Hebei Medical University, 383 Ziqiang Road, Qiaoxi, Shijiazhuang, Hebei 050000, P.R. China
E-mail: guoyuexian@aliyun.com
E-mail: 37300391@hebmu.edu.cn

Key words: bladder cancer, protein quantitative trait loci, Mendelian randomization, biomarkers, drug targets

Introduction

Globally, bladder cancer is ranked as the tenth most frequently diagnosed cancer and is the thirteenth leading cause of cancer-related mortalities (1,2). According to 2024 global cancer statistics, the number of new bladder cancer cases is estimated to have exceeded 600,000 worldwide. The age-standardized incidence rate is ~6.0 cases per 100,000 individuals, showing a slow upward trend. In the same year, the number of bladder cancer-related deaths is projected to be ~220,000, with a mortality rate maintained at ~2.0 per 100,000 individuals. In recent years, with advancements in diagnostic technologies and optimization of treatment regimens, the survival rate of patients with bladder cancer has significantly improved in some regions with high levels of development (1). The survival rate of bladder cancer still requires improvement through early detection or targeted anticancer therapy (3,4). Therefore, early diagnostic biomarkers and the development of novel therapeutic targets for bladder cancer remain a focus of our research.

Human plasma proteins exhibit great potential in disease diagnosis and treatment monitoring, with several successes achieved over the decades (5,6). Previous studies have identified various proteins such as membrane proteins, α-2-macroglobulin, and SPP1 protein, as being associated with bladder cancer risk (7-9). However, research on bladder cancer still faces limitations. In particular, the investigation into proteins associated with the development and progression of bladder cancer has not been comprehensively carried out.

Large-scale proteomic investigations have led to the identification of over 18,000 protein quantitative trait loci (pQTL) that cover upwards of 4,800 proteins. Genetic variations related to the levels of multiple plasma proteins have been identified in previous pQTL studies (10-14). These research efforts provide valuable data resources for elucidating the causal role of plasma proteins in the risk of bladder cancer through Mendelian randomization (MR). MR has been widely used in studying the pathogenesis and developing preventive strategies for various cancers, effectively distinguishing the effects of genetic factors from environmental factors, and aiding researchers identify potential disease biomarkers and therapeutic targets (15,16).

In the present study, a proteome-wide MR analysis was conducted by integrating human plasma proteomics and genomics data to systematically identify biomarkers associated with bladder cancer risk. Prognostic models were constructed based on the identified genes and further validated. Single-cell expression analysis was performed to detect their expression in bladder cancer tissues. Finally, druggability evaluation was conducted to explore their potential as therapeutic targets for bladder cancer.

Materials and methods

Data acquisition. The pQTL data were obtained from the UK Biobank Pharma Proteomics Project (UKB-PPP) database (http://ukb-ppp.gwas.eu/), with baseline cohort data selected for this analysis, describing pQTLs from 34,557 participants of European ancestry (17). Outcome data were primarily derived from genome-wide association studies (GWAS) involving populations of European ancestry. Summary statistics for the training set were sourced from the FinnGen biobank database (finngen_R10_C3_BLADDER_EXALLC), including 2,193 cases and 314,193 controls, while validation set data were retrieved from the EBI database (ID no. GCST90041858), comprising 762 cases and 455,586 controls. Additionally, RNA-seq data from 431 specimens (19 normal and 412 tumor samples) were collected from the TCGA database (https://portal.gdc.cancer.gov/), and bladder cancer-related single-cell data were downloaded from the GEO database (https://www.ncbi.nlm.nih.gov/geo/) under accession no. GSE129845 (18), including 3 samples.

PQTL MR analysis. The UKB-PPP characterized the plasma proteomics features of UKB participants. GWAS-based proteomics studies (17) were used to extract relevant causal relationships in pQTLs from the outcome summary data, by selecting single nucleotide polymorphisms (SNPs) associated with each gene at a genome-wide significance threshold ($P<10^{-6}$) as potential instrumental variables (IVs). While the genome-wide significance threshold is typically set at $P<1x10^{-8}$, relaxing it to $P<1x10^{-6}$ is considered acceptable in specific scenarios, such as candidate gene association analysis or fine-mapping analyses including sensitivity analysis focused on specific loci. When the research objective is exploratory analysis (rather than strict causal inference), this threshold increases the number of IVs and avoids missing potential associations. The LD between SNPs was calculated, retaining only SNPs with R2<0.001 (clumping window size=10,000 kb), and weak instruments with F>10 were excluded. Notably, four statistical methods were used to assess the reliability of causal relationships: Inverse Variance Weighted (IVW) (19), MR Egger (20), Weighted Median (21), and Weighted Mode (22). If only one SNP was present in the causal relationship, the Wald ratio method was used. The reliability of the identified causal relationships was verified using leave-one-out analysis.

Colocalization analysis. The coloc method (23) was used with expression quantitative trait locus (eQTL) summary data and bladder cancer GWAS data for colocalization analysis. The posterior probability was calculated for the 100-kilobase region around the index SNP. In coloc results, H3 represents the posterior probability that two traits (gene expression and bladder cancer) are associated but have different causal variants; H4 represents the posterior probability that two traits are associated and share a single causal variant. SNP.PP.H4 >0.95 was used as the colocalization threshold.

GSEA enrichment analysis. GSEA (24) is a method that utilizes predefined gene sets. It ranks genes according to the differential expression levels between two sample classes and then determines whether these predefined gene sets are over, represented at either the top or bottom of the ranking. In the present study, GSEA was employed to contrast the signaling pathways in the high-expression and low-expression groups. This was performed to investigate the molecular mechanisms underlying key genes in the 2 patient groups. The number of permutations was configured as 1,000 and the permutation type was designated as phenotype.

Tumor mutation burden (TMB) and microsatellite instability (MSI) data analysis. TMB is characterized as the cumulative count of somatic gene coding inaccuracies, including base substitutions, insertions, or deletions, identified per million bases. In the present research, the determination of TMB for each tumor sample involved calculating the mutation frequency and the number of mutations relative to the exome length. Specifically, TMB was used by dividing the number of non-synonymous mutation sites by the total length of the protein-coding region (25).

Nomogram model construction. A nomogram was developed through regression analysis, incorporating gene expression levels and clinical symptoms. This nomogram visually represents the relationships between variables within the prediction model by means of scaled lines plotted on a single plane. A multivariate regression model was constructed and the contribution of each influencing factor to the outcome variable (regression coefficient) was used to assign scores to each level of each influencing factor. The scores were summed to obtain a total score, from which the predicted value was calculated.

Drug sensitivity analysis. Using the largest pharmacogenomics database (GDSC; https://www.cancerrxgene.org/), the R package 'pRRophetic' (26) was used to predict chemotherapy sensitivity for each tumor sample. Regression methods were used to obtain IC_{50} estimates for each specific chemotherapy drug treatment, and 10-fold cross-validation was performed on the GDSC training set to verify regression and prediction

accuracy. All parameters were set to default values, including the removal of batch effects with 'combat' and averaging of replicated gene expression values.

Single-cell analysis. First, the Seurat package (27) was employed to read the expression profiles. Genes with low expression were filtered out based on the criteria: nFeature_RNA >50 and percent.mt <15. Subsequently, the data underwent normalization and scaling, followed by processing using principal component analysis (PCA). The ElbowPlot function was used to ascertain the optimal number of principal components. To visualize the positions of each cluster, t-distributed Stochastic Neighbor Embedding (28) analysis was carried out. Annotation of the clusters was performed using the celldex package (29), enabling the identification of cell types that are significantly associated with the occurrence of the disease. Each subunit of single cells was annotated using the R package SingleR (30).

Disease gene co-expression network. Disease-related genes were obtained from the GeneCards database (https://www.genecards.org/). Genes with high relevance scores were selected, and a correlation analysis was conducted to explore the co-expression network between key genes and disease-related genes.The Pearson correlation method was used for the statistical analysis.

Cell culture. The immortalized cells of human ureteral epithelium (SV-HUC-1), and human bladder cancer cell lines (T24, 5637, UMUC3, J82) were obtained from the American Type Culture Collection (ATCC). SV-HUC-1 cells were cultured in F-12K medium (Gibco; Thermo Fisher Scientific, Inc.). T24, 5637, UMUC3, and J82 cells were cultured in RPMI-1640 medium (Gibco; Thermo Fisher Scientific, Inc.). All media were supplemented with 10% fetal bovine serum (FBS; Corning, Inc.). The cells were incubated in a humidified atmosphere containing 5% CO_2 at 37˚C. Regular observation of the structural state of the cells during cell culture and regular checks for mycoplasma contamination were performed.

Reverse transcription quantitative polymerase chain reaction (RT-qPCR). TRIzol reagent (Invitrogen; Thermo Fisher Scientific, Inc.) was utilized to extract RNA from cells and tissues. Subsequently, complementary DNA (cDNA) synthesis was carried out with a reverse transcription system (FastKing One Step RT-PCR kit; Tiangen Biotech Co., Ltd.), following the manufacturer's instructions precisely. RT-qPCR was performed in triplicate using the Applied Biosystems 7500 Real-Time PCR System (Thermo Fisher Scientific, Inc.) and SYBR Green PCR Master Mix (TransStart® Top Green qPCR SuperMix; TransGen Biotech Co., Ltd.) on 96-well optical plates according to the manufacturer's instructions. The thermocycling conditions were as follows: Pre-denaturation at 95˚C for 3 min, denaturation at 95˚C for 30 sec, annealing extension at 60˚C for 30 sec, deformation and annealing extension for 40 cycles. The dissolution curve was increased by 0.5˚C every 2 cycles to 95˚C. The results were normalized to the endogenous control, β-actin. The primers used are listed in Table SI. The $2^{-\Delta\Delta Cq}$ method was used for quantification (31).

Statistical analysis. Reliable MR analysis is based on three assumptions: i) Relevance assumption (instrumental variables are closely related to the exposure but not directly related to the outcome); ii) independence assumption (instrumental variables are not related to confounding factors); and iii) exclusion restriction assumption (instrumental variables only affect the outcome through the exposure; when IVs can affect the outcome through other pathways, pleiotropy is present). All analyses were conducted using R language (version 4.0). Continuous variables were compared using paired and unpaired Student's t-test, or one-way ANOVA (single-factor analysis) followed by Bonferroni's post hoc test for multiple-group comparisons. Data are presented as the mean ± standard deviation (SD) from three independent biological replicates. All statistical tests were two-sided. $P<0.05$ was considered to indicate a statistically significant difference.

Results

pQTL MR analysis in the training set. The outcome ID finngen_R10_C3_BLADDER_EXALLC, related to bladder cancer, was obtained from summary statistics of 316,386 samples (2,193 cases and 314,193 controls). Using the extract_instruments and extract_outcome_data functions, 342 pairs of gene-outcome causal relationships were extracted (Table SII). Further MR analysis identified 114 gene-pQTL-positive causal relationships (Fig. 1A; IVW, $P<0.05$). Sensitivity analysis was performed on the causal relationships of the 114 genes to verify their reliability. The results indicated that the removal of any SNP did not significantly affect the overall error lines, suggesting that the 114 causal relationships were robust.

pQTL MR analysis. To further identify key genes among the 114 pQTL genes associated with bladder cancer, the outcome ID GCST90041858 was obtained from the summary statistics of 456,348 samples related to bladder cancer (762 cases and 455,586 controls). Using the extract_instruments and extract_outcome_data functions, 22 pairs of gene-outcome causal relationships were extracted (Table SIII). Further MR analysis identified seven gene-pQTL-positive causal relationships (Fig. 1B; $P<0.05$), corresponding to the genes all-trans retinoic acid-induced differentiation factor (ATRAID), bleomycin hydrolase (BLMH), calcineurin B homologous protein 1 (CHP1), cartilage intermediate layer protein (CILP), myosin phosphatase Rho-interacting protein (MPRIP), SLIT and NTRK-like family member 2 (SLITRK2), and tripartite motif containing 25 (TRIM25). The genes ATRAID, BLMH, MPRIP, and TRIM25 were potentially associated with a low risk of bladder cancer. The genes CHP1, CILP, and SLITRK2 were potentially associated with a high risk of bladder cancer. Sensitivity analysis was performed on the causal relationships of the seven genes to verify their reliability. The results indicated that the removal of any SNP did not significantly affect the overall error lines, suggesting that the seven causal relationships were robust (Fig. 2A-G). Additionally, colocalization analysis at the pQTL-GWAS level identified two genes with colocalization SNP.PP.H4 >0.95 (Fig. 2H and I), specifically ATRAID and TRIM25.

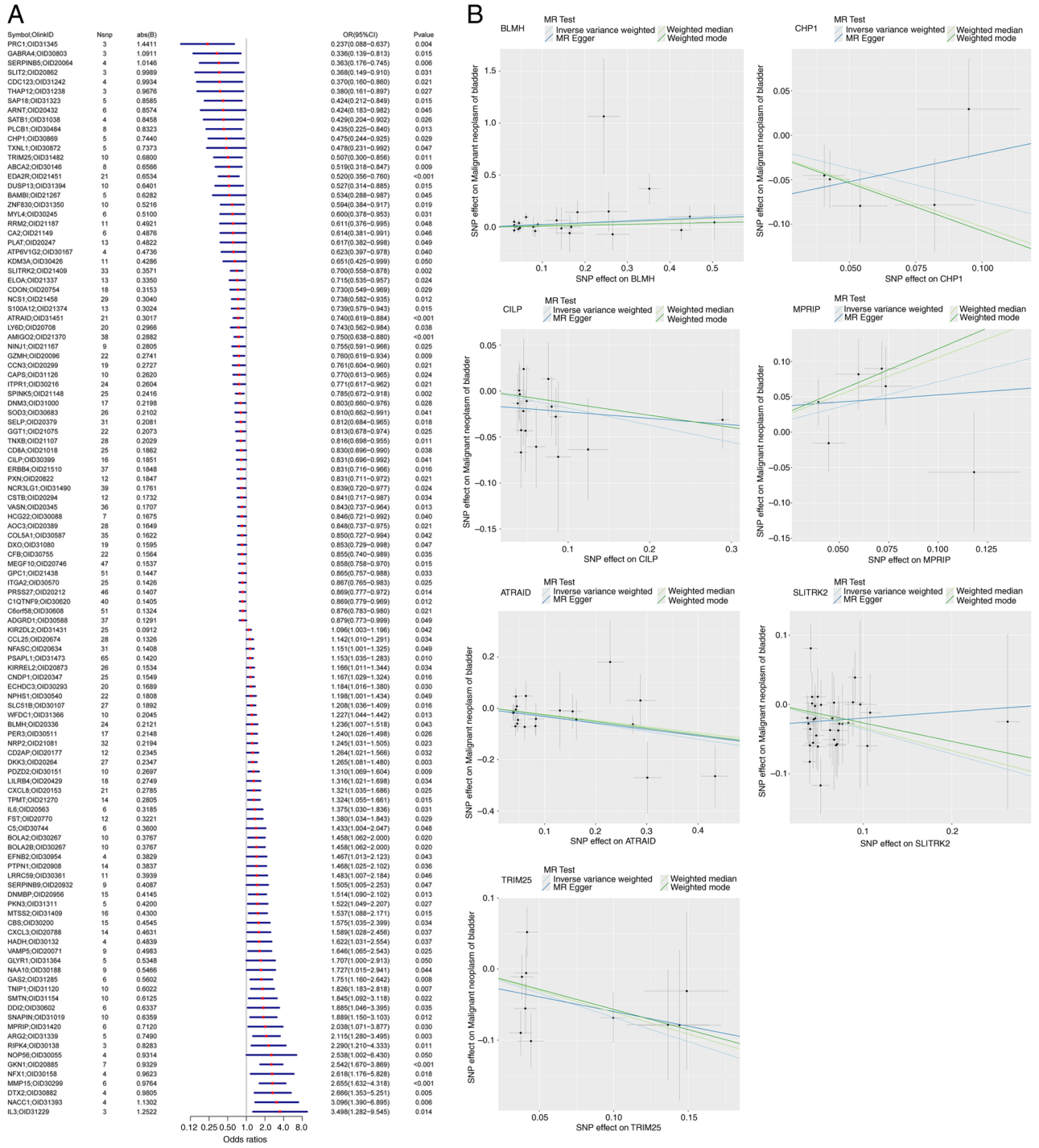

Figure 1. MR analysis screening. (A) Risk associations of 114 causal relationships identified through MR analysis. (B) Scatter plot of MR analysis for seven genes, with different colors indicating different statistical methods. The slopes of the lines represent the causal effects of each method. MR, Mendelian randomization; SNP, single nucleotide polymorphism; OR, odds ratio.

Exploration of specific signaling mechanisms related to key genes. The specific signaling pathways involved with these two key genes and their impact on disease progression-related signaling pathways were explored. GSEA results indicated that ATRAID was enriched in 'ADHERENS_JUNCTION', 'OXIDATIVE_PHOSPHORYLATION', and 'PEROXISOME' signaling pathways (Fig. 2J). TRIM25 was enriched in 'ARACHIDONIC_ACID_METABOLISM', 'CELL_CYCLE', and 'DNA_REPLICATION' signaling pathways (Fig. 2K). GSEA was further used to analyze the impact of these key genes on signaling pathways. RT-qPCR was performed to investigate the mRNA expression of ATRAID and TRIM25 in bladder cancer cell lines. The results of RT-qPCR, based on bladder cancer cell lines, demonstrated that the mRNA expression levels of ATRAID and TRIM25 were lower in tumor cell lines than in SV-HUC-1 cells (Fig. 2L and M).

Clinical predictive value of key genes. The relationship between key gene expression and clinical symptoms was analyzed. The

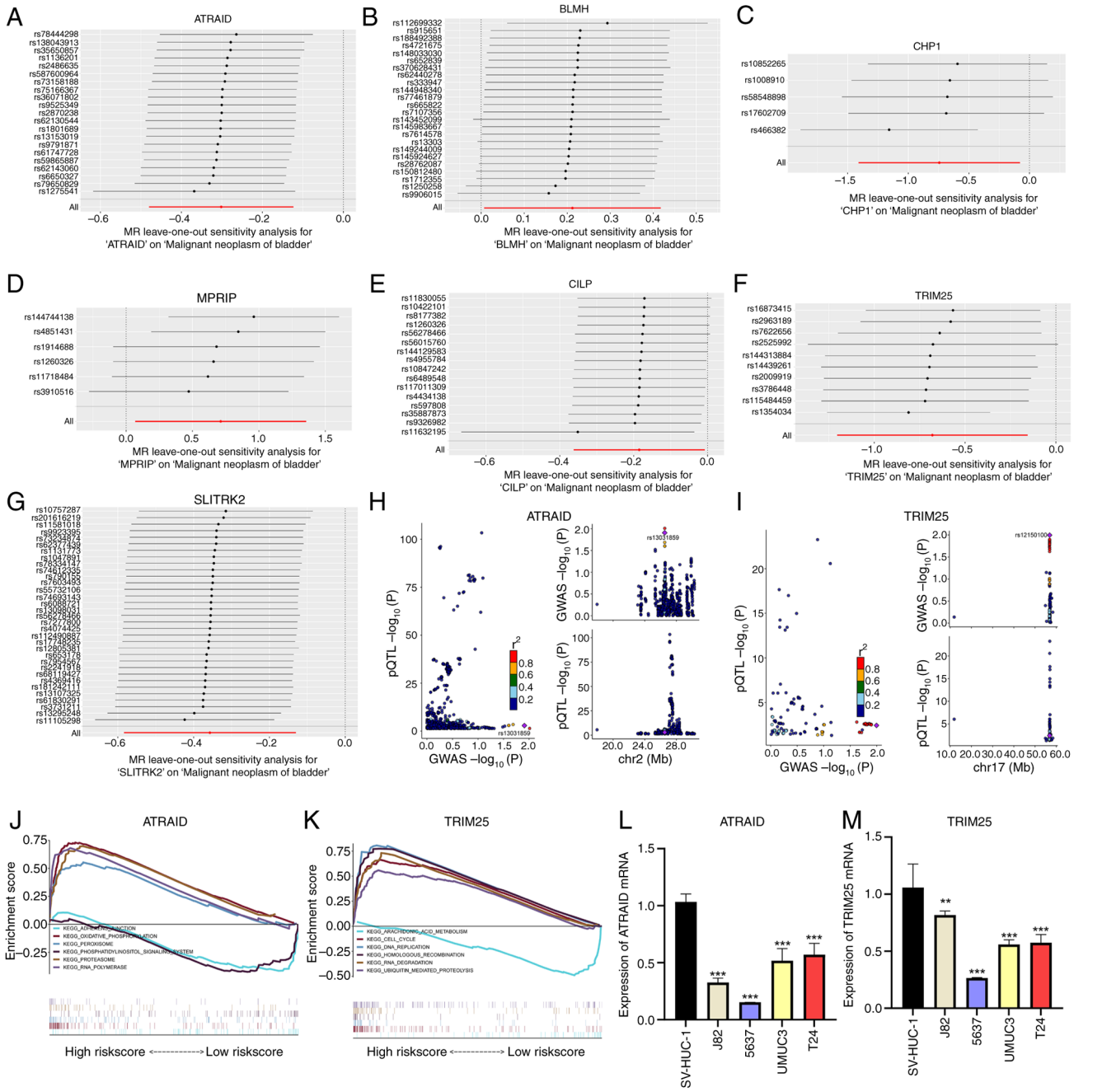

Figure 2. Key gene screening and reverse transcription-quantitative PCR validation. (A-G) Forest plots of leave-one-out analysis for SNPs corresponding to the seven genes. (H and I) Associations between SNPs of ATRAID and TRIM25 with the disease, where each point indicates a statistically significant SNP-disease association. The x-axis represents the P-value of GWAS, and the y-axis represents the P-value of the pQTL analysis. (J and K) KEGG signaling pathways involving ATRAID and TRIM25, including genes involved in pathway regulation. (L and M) mRNA expression levels of ATRAID and TRIM25 in bladder cancer cell lines. **P<0.01 and ***P<0.001. SNP, single nucleotide polymorphism; ATRAID, all-trans retinoic acid-induced differentiation factor; TRIM25, tripartite motif containing 25; GWAS, genome-wide association studies; pQTL, protein quantitative trait loci; KEGG, Kyoto, Encyclopedia of Genes and Genomes.

analysis revealed a significant difference between ATRAID and the sex of patients (Fig. 3A-H), and a significant difference between TRIM25 and the M stage of patients (Fig. 3I-P). These findings may provide guidance and support for disease diagnosis and treatment, drug development, and disease mechanism research.

Mutation profile and differences in TMB/MSI of key genes. Processed SNP-related data for bladder cancer were downloaded and the top 30 genes were selected with high mutation frequency for display, comparing the differences in mutated genes between the two groups of patients. Using the R package ComplexHeatmap, a mutation landscape map was plotted. The results revealed that there was a significant difference in the mutation frequency of AT-rich interaction domain 1 (ARID1A) between patients with high and low ATRAID expression (P=0.005), with a higher mutation proportion of ARID1A in the high-expression group (Fig. 4A). Similarly, significant differences in mutation frequencies of ARID1A

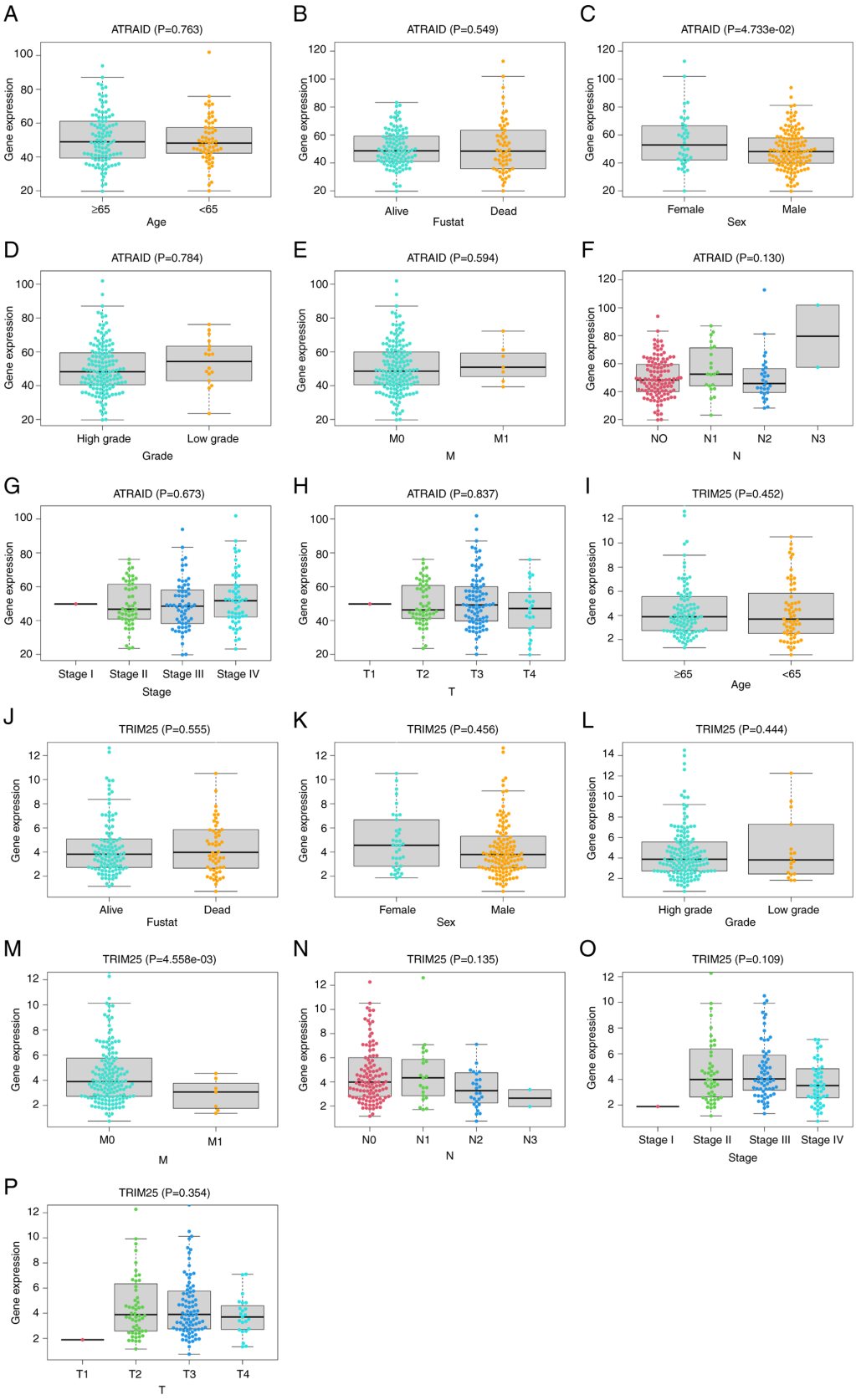

Figure 3. Association analysis with clinical indicators. (A-H) Association analysis between ATRAID and clinical indicators. (I-P) Association analysis between TRIM25 and clinical indicators. ATRAID, all-trans retinoic acid-induced differentiation factor; TRIM25, tripartite motif containing 25.

(P=0.036), microtubule-actin crosslinking factor 1 (MACF1; P=0.010), spectrin repeat containing nuclear envelope protein 2 (SYNE2; P=0.026), and CREB binding lysine acetyltransferase (CREBBP; P<0.001) were also observed between subgroups based on TRIM25 expression. The high TRIM25-expression group had a higher

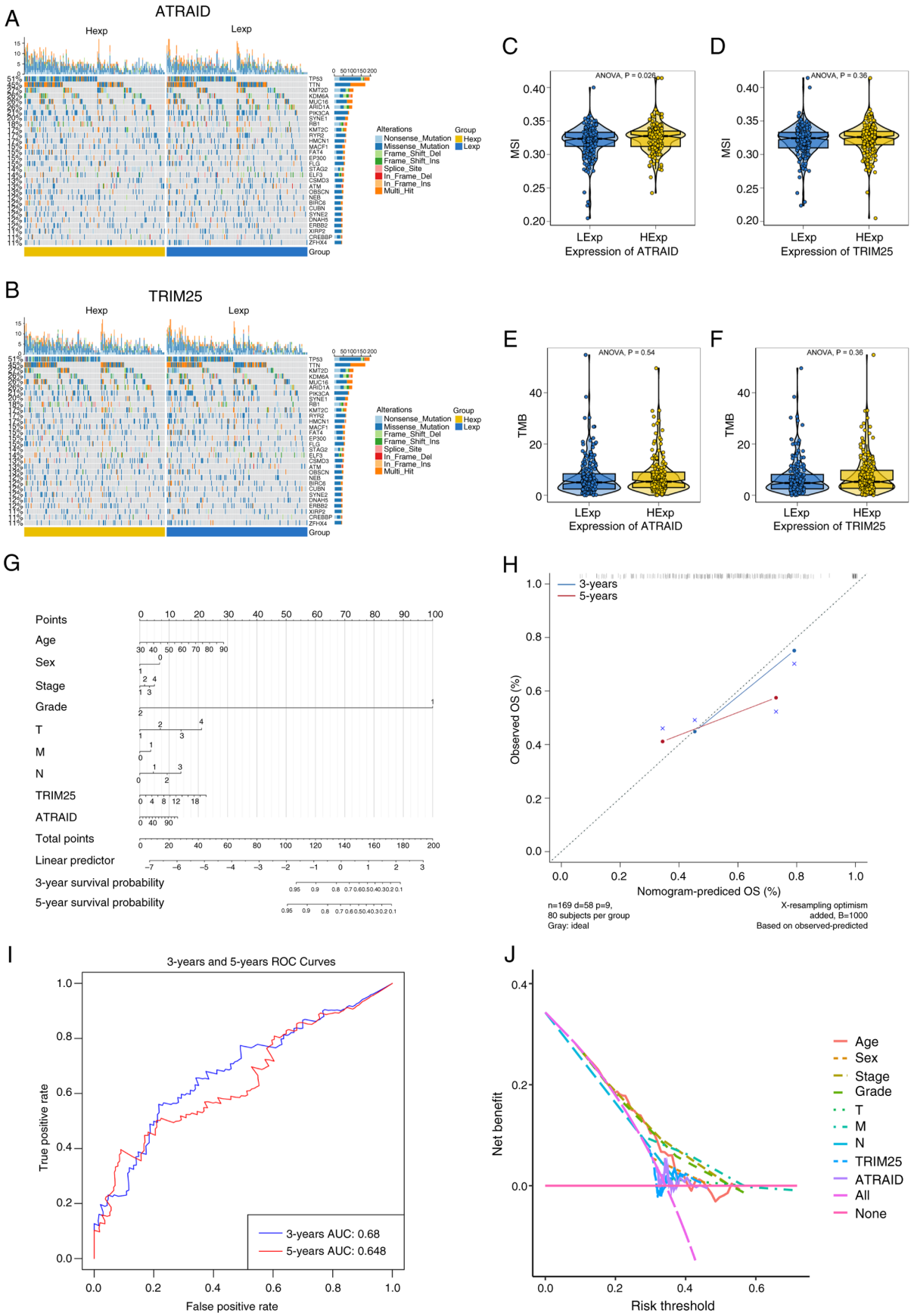

Figure 4. Mutational landscape of key genes, differences in TMB/MSI, and construction of the Nomogram model. (A and B) SNP-related data of bladder cancer, showing the top 30 genes with high mutation frequencies in 2 patient groups. (C-F) Differences in MSI and TMB between ATRAID and TRIM25. (G) Column chart of the key gene model. (H) Prediction analysis of OS for 3 and 5 years. (I and J) ROC curve and decision curve analysis. TMB, tumor mutation burden; MSI, microsatellite instability; SNP, single nucleotide polymorphism; ATRAID, all-trans retinoic acid-induced differentiation factor; TRIM25, tripartite motif containing 25; OS, overall survival; ROC, receiver operating characteristic; LExp; low expression; HExp, high expression; AUC, area under the curve.

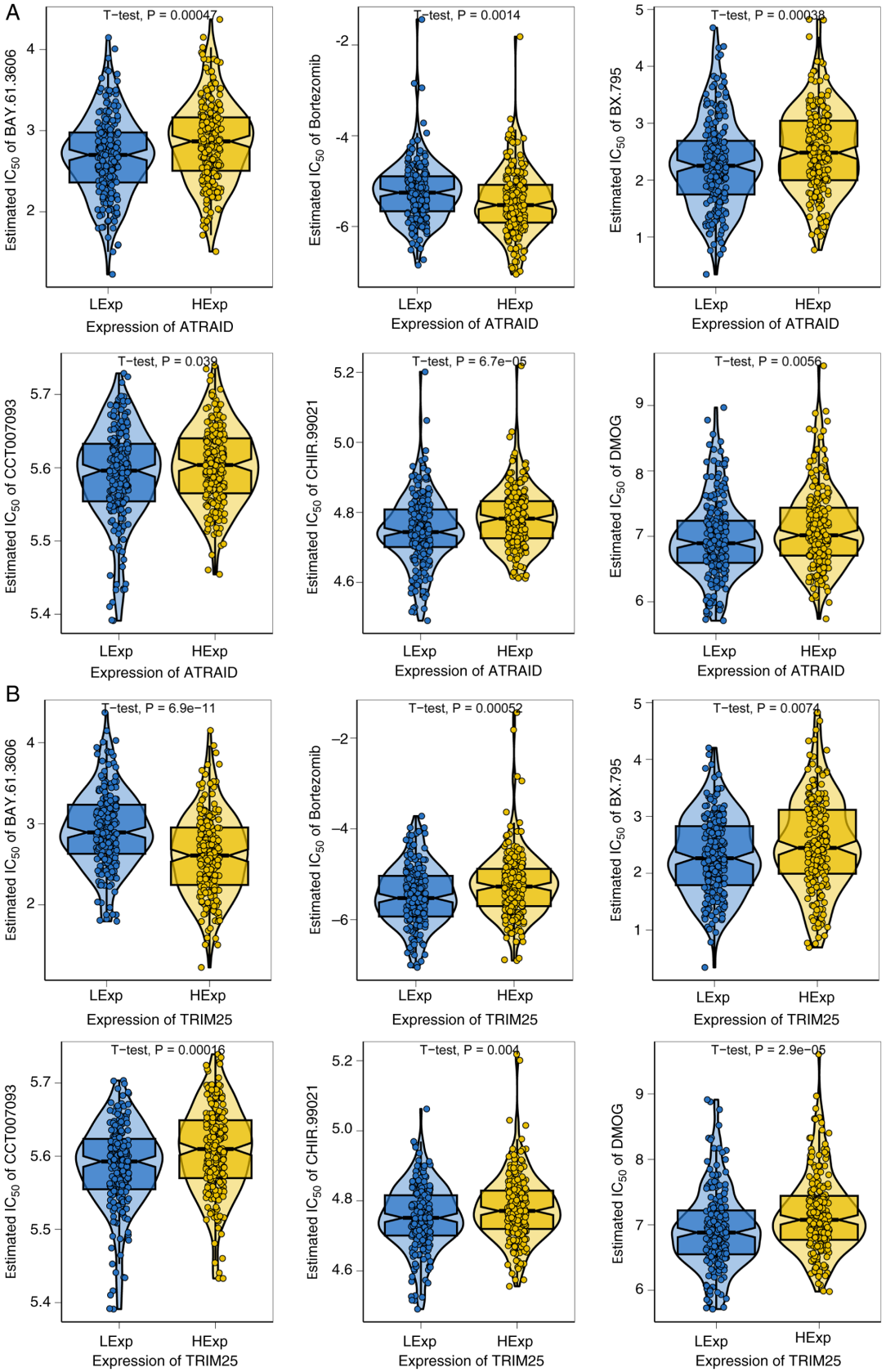

Figure 5. Drug sensitivity analysis. Sensitivity analysis of (A) ATRAID and (B) TRIM25 to chemotherapy drugs. ATRAID, all-trans retinoic acid-induced differentiation factor; TRIM25, tripartite motif containing 25; LExp; low expression; HExp, high expression; IC50, half maximal inhibitory concentration.

mutation proportion of ARID1A, MACF1, SYNE2, and CREBBP compared with the low TRIM25-expression group (Fig. 4B). The relationship between the two key genes and common immunotherapy-related tumor markers were further explored, revealing the relationship between TMB and MSI in the high- and low-expression groups

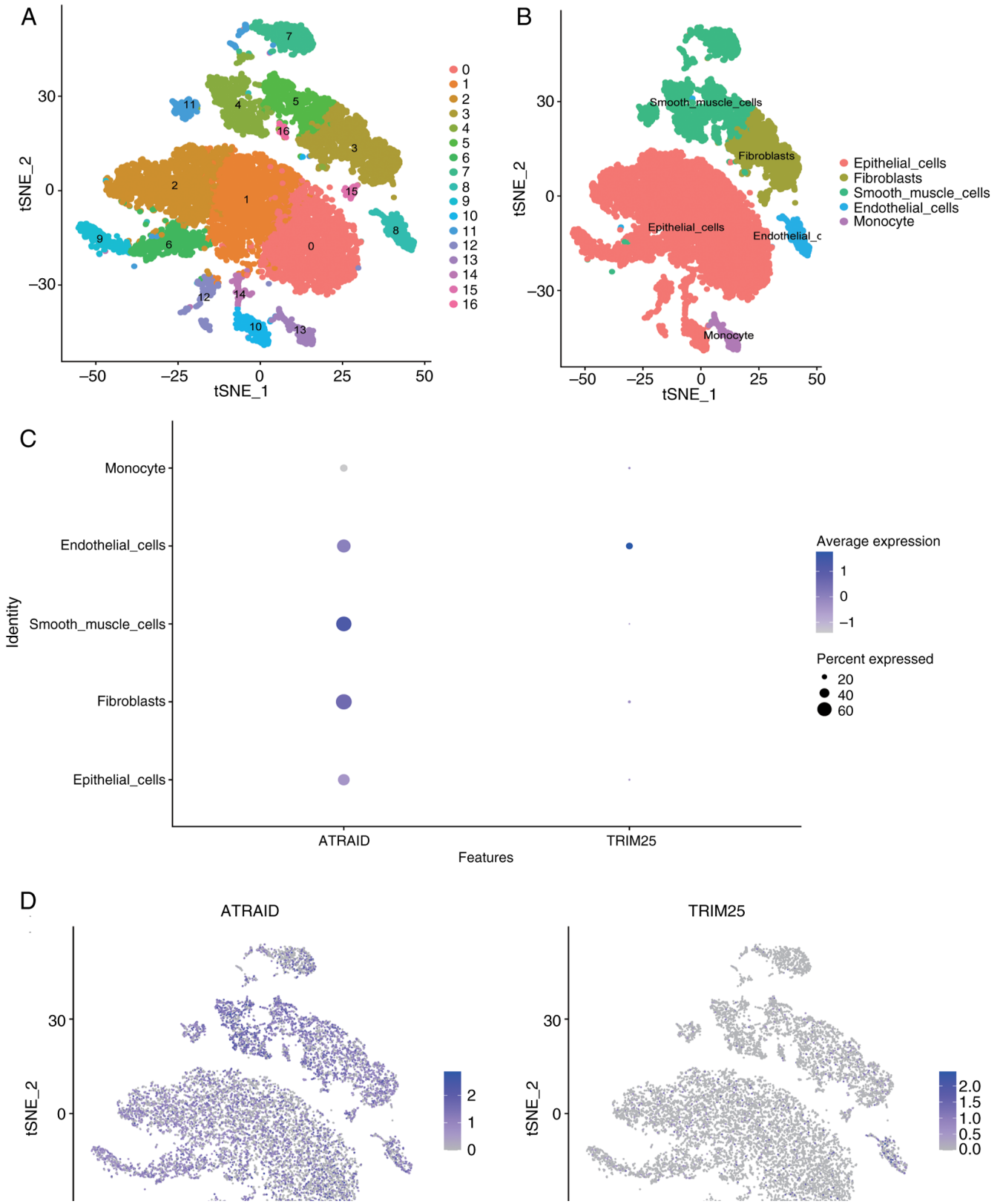

Figure 6. Expression of key genes at the single-cell level. (A) Clustering of cells into 17 clusters based on principal component analysis using the t-SNE algorithm. (B) Cell annotation of the 17 clusters, annotated into five cell types, namely Epithelial_cells, Fibroblasts, Smooth_muscle_cells, Endothelial_cells. (C and D) Expression profiles of key genes in cells. t-SNE, t-distributed Stochastic Neighbor Embedding; ATRAID, all-trans retinoic acid-induced differentiation factor; TRIM25, tripartite motif containing 25.

of key genes (Fig. 4C-F). The results indicated a statistically significant relationship between ATRAID and MSI (Fig. 4C).

Nomogram model construction. The expression levels of key genes were used to present the results of the regression analysis in the form of a nomogram. The regression analysis results

indicated that various indicators of bladder cancer, along with the distribution of key gene expression, contributed to different extents in the overall scoring process (Fig. 4G). A predictive analysis for the 3 and 5-year overall survival (OS) periods was also conducted. The results indicated that the predicted OS closely matched the observed OS, demonstrating the good predictive performance of the nomogram model. In the calibration curve, the data points in blue (3-year) and red (5-year) are both closely distributed along the diagonal line, indicating that the predicted OS aligns well with the observed OS (Fig. 4H). In the receiver operating characteristic (ROC) curve, the area under the curve (AUC) for the 3-year OS prediction was 0.68, and the AUC for the 5-year OS prediction was 0.648. Although these AUC values were not particularly high, they indicate that the model has a certain ability to distinguish between the 3 and 5-year survival outcomes of patients (Fig. 4I). In the decision curve, the purple line representing the integration of key genes and clinical indicators ('All') exhibited a higher net benefit than lines incorporating only partial factors or no factors (Fig. 4J). These findings suggest that the nomogram model constructed by combining the clinical indicators and key gene expression levels (corresponding to the 'All' curve) can provide greater net benefits to patients accross appropriate risk thresholds in real-world clinical decision-making.

Drug sensitivity analysis. Early-stage bladder cancer is effectively treated with surgery combined with chemotherapy (32). The present study used drug sensitivity data from the GDSC database and the R package 'pRRophetic' to predict the chemotherapy sensitivity of each tumor sample, and further explored the sensitivity to common chemotherapy drugs. The results indicated that the two key genes, ATRAID and TRIM25, were significantly associated with sensitivity to BAY.61.3606, bortezomib, BX.795, CCT007093, CHIR.99021, and DMOG. High ATRAID expression was associated with increased resistance of bladder cancer cells to BAY.61.3606, BX.795, CCT007093, CHIR.99021, and DMOG (higher IC_{50} values indicate a need for higher drug concentrations to inhibit 50% of cells), while enhancing sensitivity to bortezomib (Fig. 5A). Conversely, high TRIM25 expression led to increased resistance to bortezomib, BX.795, CCT007093, CHIR.99021, and DMOG, but enhanced sensitivity to BAY.61.3606 (Fig. 5B).

Expression of key genes at the single-cell level. The analysis of the present study included expression profiles from three bladder cancer-related tissue samples. Using the FindClusters function from the Seurat package, 17 subtypes were identified (Fig. 6A). The R package SingleR was used to annotate each subtype, identifying 17 clusters into five cell types: Epithelial_ cells, Fibroblasts, Smooth_muscle_cells, Endothelial_cells, and Monocytes (Fig. 6B). The expression of the two key genes in cell subtypes was analyzed and the results using bubble plots and scatter plots are displayed (Fig. 6C and D). The findings revealed that ATRAID and TRIM25 were expressed in multiple cell types, but their expression was more widespread or higher in certain cells (such as epithelial cells and fibroblasts). Multiple key genes were found to be co-expressed with tumor genes. Co-expression relationships (including both positive and negative co-expression) reflect the correlation trends in expression levels between genes. When two genes exhibit positive co-expression, their expression levels tend to change in the same direction across samples. Apoptosis-associated transcript in bladder cancer (AATBC) exhibited a negative co-expression association with both the ATRAID and TRIM25 genes (Fig. S1A and B). Fibroblast growth factor receptor 3 (FGFR3) was positively co-expressed with ATRAID and negatively co-expressed with TRIM25 (Fig. S1C and D). Hras proto-oncogene, GTPase (HRAS) was positively co-expressed with both ATRAID and TRIM25 (Figs. S1E and S2A). RB transcriptional corepressor 1 (RB1) was positively co-expressed with ATRAID and negatively expressed with TRIM25 (Fig. S2B and C). Tumor ptotein 53 (TP53) was positively co-expressed with ATRAID and negatively expressed with TRIM25 (Fig. S2D and E). Positive co-expression between two genes may indicate their involvement in the same biological process or signaling pathway, achieving functional coordination through synergistic expression. Alternatively, one gene may act as an upstream regulatory factor for the other. By contrast, negative co-expression of two genes, may reflect opposing roles in biological processes, an antagonistic relationship within a shared pathway, or mutual inhibitory regulation.

Discussion

In the present study, seven plasma proteins were detected and the gene expression levels of these proteins were found to be significantly associated with the risk of bladder cancer. Among them, the genes ATRAID and TRIM25 had a probability >0.95 of affecting the same phenotype in both pQTL and GWAS data, suggesting a high likelihood that these two genes are involved in the same biological pathway. The present study identified novel biomarkers for bladder cancer, which may provide new insights into the genetics and pathogenesis of bladder cancer.

ATRAID, also known as APR3, is a gene associated with apoptosis (33,34). Located on human chromosome 2p22.3, it can affect the cell cycle by altering cyclin D1 expression, thereby influencing malignant tumor occurrence and growth, and promoting cell differentiation (35). In the present study, its potential as a diagnostic marker for bladder cancer was identified, suggesting a suppressive role in the development of bladder cancer. However, previous studies have found increased expression of ATRAID in ovarian cancer, cervical cancer, and lung adenocarcinoma, suggesting an oncogenic role (35-37), although no studies, to the best of the authors' knowledge, have yet been conducted on ATRAID in bladder cancer. Pathway enrichment analysis of ATRAID in the present study revealed significant enrichment in adhesion function and oxidative stress. Li *et al* (33) similarly found that upregulation of APR3 expression in ARPE-19 cells significantly increased intracellular reactive oxygen species (ROS) levels and altered mitochondrial morphology, promoting cell oxidative stress by affecting mitochondrial function. ATRAID may also exert its effects in bladder cancer through similar oxidative stress pathways.

In the analysis of the relationship between ATRAID and clinical characteristics, it was determined that the expression of ATRAID was lower in male patients than in female patients. It was speculated that this difference may be related to sex

chromosome-associated genes regulating ATRAID, and it is also possible that sex hormones such as estrogen, progesterone, and testosterone may affect the expression of ATRAID. These findings suggest a potential direction for future research. In immune infiltration analysis, high expression of ATRAID was significantly positively associated with MSI status, indicating its important role in MSI tumors and possibly serving as a novel therapeutic target.

TRIM25 is an E3 ubiquitin ligase confirmed to be an RNA-binding protein (RBP) through its spry domain, and it plays a crucial role in gene regulation, controlling cell proliferation, and cancer cell migration (38-40). The regulation of TRIM25 in tumors is largely through regulation of the endoplasmic reticulum (ER), which can regulate apoptosis of tumors through the IRE1-JNK signal, upregulating the unfolded protein response and ER-associated degradation pathways (41,42). TRIM25 has been shown to play a role in the development of colon cancer, hepatocellular carcinoma, endometrial cancer, gastric cancer, prostate cancer, lung cancer, breast cancer, ovarian cancer, and renal cancer (43-53). Although several studies have explored the role of TRIM25 in bladder cancer, research on its role in this cancer type remains limited and requires further investigation (54-56). Pathway enrichment analysis of TRIM25 in the present study showed significant enrichment in 'ARACHIDONIC_ACID_METABOLISM', 'CELL_CYCLE', and 'DNA_REPLICATION' pathways. The enrichment of TRIM25 in the cell cycle pathway indicated its potential role in regulating cell cycle progression.

In the analysis of the relationship between TRIM25 and clinical characteristics, it was found that the expression of TRIM25 was lower in patients with distant metastases than in those without, which may indicate that the expression of TRIM25 is related to the occurrence of tumor metastasis, possibly exerting an inhibitory effect in the invasion and metastasis process of bladder cancer cells.

By combining ATRAID and TRIM25 with patient clinical data, bladder cancer 3 and 5-year survival prediction models were constructed, with model AUCs of 0.68 and 0.648, respectively. The 3 and 5-year prognostic models constructed in the present study demonstrated relatively high predictive accuracy, which can assist clinicians in predicting the prognosis of individual patients. For patients predicted to have a shorter survival time, more aggressive treatment options can be considered, while for those predicted with a longer predicted survival, more conservative treatment strategies can be selected.

Drug sensitivity analysis of ATRAID and TRIM25 revealed that high expression of ATRAID was associated with increased resistance of bladder cancer cells to BAY.61.3606, BX.795, CCT007093, CHIR.99021, and DMOG (higher IC_{50} values indicate higher drug concentrations required to inhibit 50% of cells), while enhancing sensitivity to bortezomib. Conversely, high expression of TRIM25 led to increased resistance to bortezomib, BX.795, CCT007093, CHIR.99021, and DMOG, but enhanced sensitivity to BAY.61.3606. From the perspective of drug sensitivity, these findings suggest that the expression levels of ATRAID and TRIM25 may serve as drug response prediction indicators (patients with high expression may exhibit poorer efficacy to these drugs). This implies that the expression levels of these two genes may influence the response of tumor cells to these drugs, and the drugs may regulate bladder cancer by affecting signaling pathways associated with ATRAID and TRIM25. Further investigation of these associations could improve our understanding of tumor drug response mechanisms and provide novel insights and strategies for personalized therapy.

ATRAID was mainly expressed in 'Fibroblasts' and 'Smooth_muscle_cells', indicating that ATRAID may play an important role in tumor stromal remodeling or microenvironment regulation. TRIM25 was mainly expressed in 'Endothelial_cells', indicating that TRIM25 may play an important role in encoding vascular growth factors and regulating vascular maturation and stability.

In the present study, the association between plasma protein biomarkers and bladder cancer risk was comprehensively explored. A two-stage screening MR design was employed, which is characterized by a large sample size and a minimal likelihood of reverse causation and confounding bias. The consistency of multiple rigorous analysis results confirms the robustness of the findings of the present study. By screening ATRAID and TRIM25, a predictive model was constructed to effectively predict the 3 and 5-year survival rates. The small sample size in the single-cell analysis of bladder cancer may fail to accurately reflect cellular heterogeneity, which is also one of the limitations of the present study. In addition, only qPCR was used to verify the RNA expression levels of the two genes, ATRAID and TRIM25. Verification at the protein level using western blotting and immunohistochemistry has yet to be carried out. Similarly, the functional verification of the ATRAID and TRIM25 genes in bladder cancer and the exploration of the mechanisms by which these two genes participate in the occurrence and development of bladder cancer have not been performed. Subsequently, bladder cancer cell lines with knockdown and overexpression of the ATRAID and TRIM25 genes will be constructed for functional exploration. Furthermore, the specific mechanisms affected by these two genes will be investigated, particularly in the direction of bladder cancer drug resistance. In addition, an in-depth research on their mechanisms will be conducted, so as to provide valuable insights for future studies on drug resistance in bladder cancer. In the present study, ATRAID and TRIM25 were identified as biomarkers associated with bladder cancer risk. These findings not only provide novel perspectives on the causes of bladder cancer, but also offer potential targets for the development of innovative biomarkers and therapeutic drugs against bladder cancer.

Acknowledgements

Not applicable.

Funding

The present study was supported by the Central Government Guiding Local Funds for Science and Technology Development (grant no. 236Z7710G), and the Peking University First Hospital-Miyun Hospital Joint Program (grant no. 2023-study029-001).

Availability of data and materials

The data generated in the present study may be requested from the corresponding author.

Authors' contributions

WG, YL, ZF, ZG, YaG, XJ, YJ and YuG conceptualized and designed the present study. WG, YL, ZF, ZG, YaG, XJ, YJ and YuG provided administrative support. WG, YL and ZF conducted the collation of public data. WG, YL and ZF collected and assembled the data of the present study. WG, YL and ZF analyzed and interpretated the data. WG and YuG confirm the authenticity of all the raw data. All authors assisted with the writing of the present study, and read and approved the final manuscript.

Ethics approval and consent to participate

The present study was carried out in compliance with the Declaration of Helsinki (revised in 2013). Additionally, the present study was approved (approval no. 2023-029-001) by the Ethics Committee of Peking University First Hospital-Miyun Hospital (Beijing, China).

Patient consent for publication

Not applicable.

Competing interests

The authors declare that they have no competing interests.

References

1. Zhang Y, Rumgay H, Li M, Yu H, Pan H and Ni J: The global landscape of bladder cancer incidence and mortality in 2020 and projections to 2040. J Glob Health 13: 04109, 2023.
2. Sung H, Ferlay J, Siegel RL, Laversanne M, Soerjomataram I, Jemal A and Bray F: Global cancer statistics 2020: GLOBOCAN estimates of incidence and mortality worldwide for 36 cancers in 185 countries. CA Cancer J Clin 71: 209-249, 2021.
3. Peng M, Chu X, Peng Y, Li D, Zhang Z, Wang W, Zhou X, Xiao D and Yang X: Targeted therapies in bladder cancer: Signaling pathways, applications, and challenges. MedComm (2020) 4: e455, 2023.
4. Thomas J and Sonpavde G: Molecularly targeted therapy towards genetic alterations in advanced bladder cancer. Cancers (Basel) 14: 1795, 2022.
5. Anderson NL and Anderson NG: The human plasma proteome: History, character, and diagnostic prospects. Mol Cell Proteomics 1: 845-867, 2002.
6. Suhre K, McCarthy MI and Schwenk JM: Genetics meets proteomics: Perspectives for large population-based studies. Nat Rev Genet 22: 19-37, 2021.
7. Roslan A, Sulaiman N, Mohd Ghani KA and Nurdin A: Cancer-associated membrane protein as targeted therapy for bladder cancer. Pharmaceutics 14: 2218, 2022.
8. Sarafidis M, Lambrou GI, Zoumpourlis V and Koutsouris D: An integrated bioinformatics analysis towards the identification of diagnostic, prognostic, and predictive key biomarkers for urinary bladder cancer. Cancers (Basel) 14: 3358, 2022.
9. Kojima T, Kawai K, Miyazaki J and Nishiyama H: Biomarkers for precision medicine in bladder cancer. Int J Clin Oncol 22: 207-213, 2017.
10. Pietzner M, Wheeler E, Carrasco-Zanini J, Cortes A, Koprulu M, Wörheide MA, Oerton E, Cook J, Stewart ID, Kerrison ND, *et al*: Mapping the proteo-genomic convergence of human diseases. Science 374: eabj1541, 2021.
11. Ferkingstad E, Sulem P, Atlason BA, Sveinbjornsson G, Magnusson MI, Styrmisdottir EL, Gunnarsdottir K, Helgason A, Oddsson A, Halldorsson BV, *et al*: Large-scale integration of the plasma proteome with genetics and disease. Nat Genet 53: 1712-1721, 2021.
12. Zhang J, Dutta D, Köttgen A, Tin A, Schlosser P, Grams ME, Harvey B; CKDGen Consortium; Yu B, Boerwinkle E, *et al*: Plasma proteome analyses in individuals of European and African ancestry identify cis-pQTLs and models for proteome-wide association studies. Nat Genet 54: 593-602, 2022.
13. Sun BB, Maranville JC, Peters JE, Stacey D, Staley JR, Blackshaw J, Burgess S, Jiang T, Paige E, Surendran P, *et al*: Genomic atlas of the human plasma proteome. Nature 558: 73-79, 2018.
14. Suhre K, Arnold M, Bhagwat AM, Cotton RJ, Engelke R, Raffler J, Sarwath H, Thareja G, Wahl A, DeLisle RK, *et al*: Connecting genetic risk to disease end points through the human blood plasma proteome. Nat Commun 8: 14357, 2017.
15. Davies NM, Holmes MV and Davey Smith G: Reading mendelian randomisation studies: A guide, glossary, and checklist for clinicians. BMJ 362: k601, 2018.
16. Xin J, Gu D, Chen S, Ben S, Li H, Zhang Z, Du M and Wang M: SUMMER: A Mendelian randomization interactive server to systematically evaluate the causal effects of risk factors and circulating biomarkers on pan-cancer survival. Nucleic Acids Res 51 (D1): D1160-D1167, 2023.
17. Sun BB, Chiou J, Traylor M, Benner C, Hsu YH, Richardson TG, Surendran P, Mahajan A, Robins C, Vasquez-Grinnell SG, *et al*: Plasma proteomic associations with genetics and health in the UK Biobank. Nature 622: 329-338, 2023.
18. Yu Z, Liao J, Chen Y, Zou C, Zhang H, Cheng J, Liu D, Li T, Zhang Q, Li J, *et al*: Single-cell transcriptomic map of the human and mouse bladders. J Am Soc Nephrol 30: 2159-2176, 2019.
19. Burgess S, Butterworth A and Thompson SG: Mendelian randomization analysis with multiple genetic variants using summarized data. Genet Epidemiol 37: 658-665, 2013.
20. Bowden J, Davey Smith G and Burgess S: Mendelian randomization with invalid instruments: Effect estimation and bias detection through Egger regression. Int J Epidemiol 44: 512-525, 2015.
21. Bowden J, Davey Smith G, Haycock PC and Burgess S: Consistent estimation in mendelian randomization with some invalid instruments using a weighted median estimator. Genet Epidemiol 40: 304-314, 2016.
22. Hartwig FP, Davey Smith G and Bowden J: Robust inference in summary data Mendelian randomization via the zero modal pleiotropy assumption. Int J Epidemiol 46: 1985-1998, 2017.
23. Giambartolomei C, Vukcevic D, Schadt EE, Franke L, Hingorani AD, Wallace C and Plagnol V: Bayesian test for colocalisation between pairs of genetic association studies using summary statistics. PLoS Genet 10: e1004383, 2014.
24. Subramanian A, Tamayo P, Mootha VK, Mukherjee S, Ebert BL, Gillette MA, Paulovich A, Pomeroy SL, Golub TR, Lander ES and Mesirov JP: Gene set enrichment analysis: A knowledge-based approach for interpreting genome-wide expression profiles. Proc Natl Acad Sci USA 102: 15545-15550, 2005.
25. Bonneville R, Krook MA, Kautto EA, Miya J, Wing MR, Chen HZ, Reeser JW, Yu L and Roychowdhury S: Landscape of microsatellite instability across 39 cancer types. JCO Precis Oncol 2017: PO.17.00073, 2017.
26. Geeleher P, Cox N and Huang RS: pRRophetic: An R package for prediction of clinical chemotherapeutic response from tumor gene expression levels. PLoS One 9: e107468, 2014.
27. Hao Y, Hao S, Andersen-Nissen E, Mauck WM III, Zheng S, Butler A, Lee MJ, Wilk AJ, Darby C, Zager M, *et al*: Integrated analysis of multimodal single-cell data. Cell 184: 3573-3587.e29, 2021.
28. Cieslak MC, Castelfranco AM, Roncalli V, Lenz PH and Hartline DK: t-Distributed stochastic neighbor embedding (t-SNE): A tool for eco-physiological transcriptomic analysis. Mar Genomics 51: 100723, 2020.
29. Zhang Q, Yu B, Zhang Y, Tian Y, Yang S, Chen Y and Wu H: Combination of single-cell and bulk RNA seq reveals the immune infiltration landscape and targeted therapeutic drugs in spinal cord injury. Front Immunol 14: 1068359, 2023.
30. Aran D, Looney AP, Liu L, Wu E, Fong V, Hsu A, Chak S, Naikawadi RP, Wolters PJ, Abate AR, *et al*: Reference-based analysis of lung single-cell sequencing reveals a transitional profibrotic macrophage. Nat. Immunol 20: 163-172, 2019.

31. Livak KJ and Schmittgen TD: Analysis of relative gene expression data using real-time quantitative PCR and the 2(-Delta Delta C(T)) method. Methods 25: 402-408, 2001.
32. Wang W, Lu Z, Wang M, Liu Z, Wu B, Yang C, Huan H and Gong P: The cuproptosis-related signature associated with the tumor environment and prognosis of patients with glioma. Front Immunol 13: 998236, 2022.
33. Li Y, Zou X, Gao J, Cao K, Feng Z and Liu J: APR3 modulates oxidative stress and mitochondrial function in ARPE-19 cells. FASEB J: fj201800001RR, 2018 (Epub ahead of print).
34. Zhu F, Yan W, Zhao ZL, Chai YB, Lu F, Wang Q, Peng WD, Yang AG and Wang CJ: Improved PCR-based subtractive hybridization strategy for cloning differentially expressed genes. Biotechniques 29: 310-313, 2000.
35. Zhang Y, Li Q, Huang W, Zhang J, Han Z, Wei H, Cui J, Wang Y and Yan W: Increased expression of apoptosis-related protein 3 is highly associated with tumorigenesis and progression of cervical squamous cell carcinoma. Hum Pathol 44: 388-393, 2013.
36. Zhang P, Zhou C, Jing Q, Gao Y, Yang L, Li Y, Du J, Tong X and Wang Y: Role of APR3 in cancer: Apoptosis, autophagy, oxidative stress, and cancer therapy. Apoptosis 28: 1520-1533, 2023.
37. Cao HL, Gu MQ, Sun Z and Chen ZJ: miR-144-3p contributes to the development of thyroid tumors through the PTEN/PI3K/AKT pathway. Cancer Manag Res 12: 9845-9855, 2020.
38. Kwon SC, Yi H, Eichelbaum K, Föhr S, Fischer B, You KT, Castello A, Krijgsveld J, Hentze MW and Kim VN: The RNA-binding protein repertoire of embryonic stem cells. Nat Struct Mol Biol 20: 1122-1130, 2013.
39. Choudhury NR, Heikel G, Trubitsyna M, Kubik P, Nowak JS, Webb S, Granneman S, Spanos C, Rappsilber J, Castello A and Michlewski G: RNA-binding activity of TRIM25 is mediated by its PRY/SPRY domain and is required for ubiquitination. BMC Biol 15: 105, 2017.
40. Heikel G, Choudhury NR and Michlewski G: The role of Trim25 in development, disease and RNA metabolism. Biochem Soc Trans 44: 1045-1050, 2016.
41. Liu Y, Tao S, Liao L, Li Y, Li H, Li Z, Lin L, Wan X, Yang X and Chen L: TRIM25 promotes the cell survival and growth of hepatocellular carcinoma through targeting Keap1-Nrf2 pathway. Nat Commun 11: 348, 2020.
42. Rahimi-Tesiye M, Zaersabet M, Salehiyeh S and Jafari SZ: The role of TRIM25 in the occurrence and development of cancers and inflammatory diseases. Biochim Biophys Acta Rev Cancer 1878: 188954, 2023.
43. Shu XS, Zhao Y, Sun Y, Zhong L, Cheng Y, Zhang Y, Ning K, Tao Q, Wang Y and Ying Y: The epigenetic modifier PBRM1 restricts the basal activity of the innate immune system by repressing retinoic acid-inducible gene-I-like receptor signalling and is a potential prognostic biomarker for colon cancer. J Pathol 244: 36-48, 2018.
44. Li YH, Zhong M, Zang HL and Tian XF: The E3 ligase for metastasis associated 1 protein, TRIM25, is targeted by microRNA-873 in hepatocellular carcinoma. Exp Cell Res 368: 37-41, 2018.
45. Wang J, Yin G, Bian H, Yang J, Zhou P, Yan K, Liu C, Chen P, Zhu J, Li Z and Xue T: LncRNA XIST upregulates TRIM25 via negatively regulating miR-192 in hepatitis B virus-related hepatocellular carcinoma. Mol Med 27: 41, 2021.
46. Dai H, Zhao S, Xu L, Chen A and Dai S: Expression of Efp, VEGF and bFGF in normal, hyperplastic and malignant endometrial tissue. Oncol Rep 23: 795-799, 2010.
47. Dai H, Zhang P, Zhao S, Zhang J and Wang B: Regulation of the vascular endothelial growth factor and growth by estrogen and antiestrogens through Efp in Ishikawa endometrial carcinoma cells. Oncol Rep 21: 395-401, 2009.
48. Yang KS, Xu CQ and Lv J: Identification and validation of the prognostic value of cyclic GMP-AMP synthase-stimulator of interferon (cGAS-STING) related genes in gastric cancer. Bioengineered 12: 1238-1250, 2021.
49. Wang S, Kollipara RK, Humphries CG, Ma SH, Hutchinson R, Li R, Siddiqui J, Tomlins SA, Raj GV and Kittler R: The ubiquitin ligase TRIM25 targets ERG for degradation in prostate cancer. Oncotarget 7: 64921-64931, 2016.
50. Qin X, Chen S, Qiu Z, Zhang Y and Qiu F: Proteomic analysis of ubiquitination-associated proteins in a cisplatin-resistant human lung adenocarcinoma cell line. Int J Mol Med 29: 791-800, 2012.
51. Walsh LA, Alvarez MJ, Sabio EY, Reyngold M, Makarov V, Mukherjee S, Lee KW, Desrichard A, Turcan Ş, Dalin MG, *et al*: An integrated systems biology approach identifies TRIM25 as a key determinant of breast cancer metastasis. Cell Rep 20: 1623-1640, 2017.
52. Li F, Sun Q, Liu K, Zhang L, Lin N, You K, Liu M, Kon N, Tian F, Mao Z, *et al*: OTUD5 cooperates with TRIM25 in transcriptional regulation and tumor progression via deubiquitination activity. Nat Commun 11: 4184, 2020.
53. Zhenilo S, Deyev I, Litvinova E, Zhigalova N, Kaplun D, Sokolov A, Mazur A and Prokhortchouk E: DeSUMOylation switches Kaiso from activator to repressor upon hyperosmotic stress. Cell Death Differ 25: 1938-1951, 2018.
54. Tang H, Li X, Jiang L, Liu Z, Chen L, Chen J, Deng M, Zhou F, Zheng X and Liu Z: RITA1 drives the growth of bladder cancer cells by recruiting TRIM25 to facilitate the proteasomal degradation of RBPJ. Cancer Sci 113: 3071-3084, 2022.
55. Li W, Shen Y, Yang C, Ye F, Liang Y, Cheng Z, Ou Y, Chen W, Chen Z, Zou L, *et al*: Identification of a novel ferroptosis-inducing micropeptide in bladder cancer. Cancer Lett 582: 216515, 2024.
56. Eberhardt W, Nasrullah U and Pfeilschifter J: TRIM25: A global player of cell death pathways and promising target of tumor-sensitizing therapies. Cells 14: 65, 2025.

Copyright © 2025 Gao et al. This work is licensed under a Creative Commons Attribution-NonCommercial-NoDerivatives 4.0 International (CC BY-NC-ND 4.0) License.